

An extremely luminous X-ray outburst at the birth of a supernova

A. M. Soderberg^{1,2}, E. Berger^{1,2}, K. L. Page³, P. Schady⁴, J. Parrent⁵, D. Pooley⁶, X.-Y. Wang⁷, E. O. Ofek⁸, A. Cucchiara⁹, A. Rau⁸, E. Waxman¹⁰, J. D. Simon⁸, D. C.-J. Bock¹¹, P. A. Milne¹², M. J. Page⁴, J. C. Barentine¹³, S. D. Barthelmy¹⁴, A. P. Beardmore³, M. F. Bietenholz^{15,16}, P. Brown⁹, A. Burrows¹, D. N. Burrows⁹, G. Byrnes¹⁷, S. B. Cenko¹⁸, P. Chandra¹⁹, J. R. Cummings²⁰, D. B. Fox⁹, A. Gal-Yam¹⁰, N. Gehrels²⁰, S. Immler²⁰, M. Kasliwal⁸, A. K. H. Kong²¹, H. A. Krimm^{20,22}, S. R. Kulkarni⁸, T. J. Maccarone²³, P. Mészáros⁹, E. Nakar²⁴, P. T. O'Brien³, R. A. Overzier²⁵, M. de Pasquale⁴, J. Racusin⁹, N. Rea²⁶ & D. G. York²⁷

Massive stars end their short lives in spectacular explosions—supernovae—that synthesize new elements and drive galaxy evolution. Historically, supernovae were discovered mainly through their ‘delayed’ optical light (some days after the burst of neutrinos that marks the actual event), preventing observations in the first moments following the explosion. As a result, the progenitors of some supernovae and the events leading up to their violent demise remain intensely debated. Here we report the serendipitous discovery of a supernova at the time of the explosion, marked by an extremely luminous X-ray outburst. We attribute the outburst to the ‘break-out’ of the supernova shock wave from the progenitor star, and show that the inferred rate of such events agrees with that of all core-collapse supernovae. We predict that future wide-field X-ray surveys will catch each year hundreds of supernovae in the act of exploding.

Stars more massive than about eight times the mass of the Sun meet their death in cataclysmic explosions termed supernovae. These explosions give birth to the most extreme compact objects—neutron stars and black holes—and enrich their environments with heavy elements. It is generally accepted that supernovae are triggered when the stellar core runs out of fuel for nuclear burning and thus collapses under its own gravity (see ref. 1 and references therein). As the collapsing core rebounds, it generates a shock wave that propagates through, and explodes, the star.

The resulting explosion ejects several solar masses of stellar material with a mean velocity² of about 10^4 km s^{-1} , or a kinetic energy of about 10^{51} erg. Less than a solar mass of ⁵⁶Ni is synthesized in the explosion, but its subsequent radioactive decay powers¹ the luminous optical light observed to peak 1–3 weeks after the explosion. It is through this delayed signature that supernovae have been discovered both historically and in modern searches.

Although the general picture of core collapse has been recognized for many years, the details of the explosion remain unclear and most supernova simulations fail to produce an explosion. The gaps in our understanding are due to the absence of detailed observations in the first days after the explosion, and the related difficulty in detecting the weak neutrino³ and gravitational wave signatures of the explosion.

These signals offer a direct view of the explosion mechanism but require the discovery of supernovae at the time of explosion.

In this Article we describe our serendipitous discovery of an extremely luminous X-ray outburst that marks the birth of a supernova of type Ibc. Prompt bursts of X-ray and/or ultraviolet emission have been theorized^{4,5} to accompany the break-out of the supernova shock wave through the stellar surface, but their short durations (just seconds to hours) and the lack of sensitive wide-field X-ray and ultraviolet searches have prevented their discovery until now.

Our detection enables an unprecedented early and detailed view of the supernova, allowing us to infer⁶ the radius of the progenitor star, its mass loss in the final hours before the explosion, and the speed of the shock as it explodes the star. Drawing on optical, ultraviolet, radio and X-ray observations, we show that the progenitor was compact (radius $R_* \approx 10^{11}$ cm) and stripped of its outer hydrogen envelope by a strong and steady stellar wind. These properties are consistent⁷ with those of Wolf-Rayet stars, the favoured⁸ progenitors of type Ibc supernovae.

Wolf-Rayet stars are also argued⁹ to give rise to γ -ray bursts (GRBs), a related but rare class of explosions characterized by highly collimated relativistic jets. Our observations, however, indicate an ordinary spherical and non-relativistic explosion and we firmly rule out a GRB connection.

¹Department of Astrophysical Sciences, Princeton University, Ivy Lane, Princeton, New Jersey 08544, USA. ²Carnegie Observatories, 813 Santa Barbara Street, Pasadena, California 91101, USA. ³Department of Physics and Astronomy, University of Leicester, Leicester LE1 7RH, UK. ⁴Mullard Space Science Laboratory, University College London, Holmbury St Mary, Dorking, Surrey RH5 6NT, UK. ⁵Physics and Astronomy Department, Dartmouth College, Hanover, New Hampshire 03755, USA. ⁶Astronomy Department, University of Wisconsin, 475 North Charter Street, Madison, Wisconsin 53706, USA. ⁷Department of Astronomy, Nanjing University, Nanjing 210093, China. ⁸Department of Astronomy, 105-24, California Institute of Technology, Pasadena, California 91125, USA. ⁹Department of Astronomy and Astrophysics, Pennsylvania State University, University Park, Pennsylvania 16802, USA. ¹⁰Faculty of Physics, Weizmann Institute of Science, Rehovot 76100, Israel. ¹¹Radio Astronomy Laboratory, University of California, Berkeley, California 94720, USA. ¹²Steward Observatory, University of Arizona, 933 North Cherry Avenue, Tucson, Arizona 85721, USA. ¹³Department of Astronomy, University of Texas at Austin, Austin, Texas 78712, USA. ¹⁴NASA Goddard Space Flight Center, Greenbelt, Maryland 20771, USA. ¹⁵Department of Physics and Astronomy, York University, Toronto, Ontario M3J 1P3, Canada. ¹⁶Hartebeestehoeck Radio Observatory, PO Box 443, Krugersdorp, 1740, South Africa. ¹⁷Department of Physics and Astronomy, Clemson University, Clemson, South Carolina 29634, USA. ¹⁸Space Radiation Laboratory, 220-47, California Institute of Technology, Pasadena, California 91125, USA. ¹⁹Department of Astronomy, University of Virginia, PO Box 400325, Charlottesville, Virginia 22904, USA. ²⁰CRESST and NASA Goddard Space Flight Center, Greenbelt, Maryland 20771, USA. ²¹Institute of Astronomy and Department of Physics, National Tsing Hua University, Hsinchu, Taiwan. ²²Universities Space Research Association, 10211 Wincopin Circle, #500, Columbia, Maryland 21044, USA. ²³School of Physics and Astronomy, University of Southampton, Southampton SO17 1BJ, UK. ²⁴Theoretical Astrophysics, 130-33, California Institute of Technology, Pasadena, California 91125, USA. ²⁵Max-Planck-Institut für Astrophysik, D-85748 Garching, Germany. ²⁶University of Amsterdam, Astronomical Institute ‘Anton Pannekoek’, Kruislaan 403, 1098SJ, Amsterdam, The Netherlands. ²⁷Department of Astronomy and Astrophysics, University of Chicago, 5640 S. Ellis Avenue, Chicago, Illinois 60637, USA.

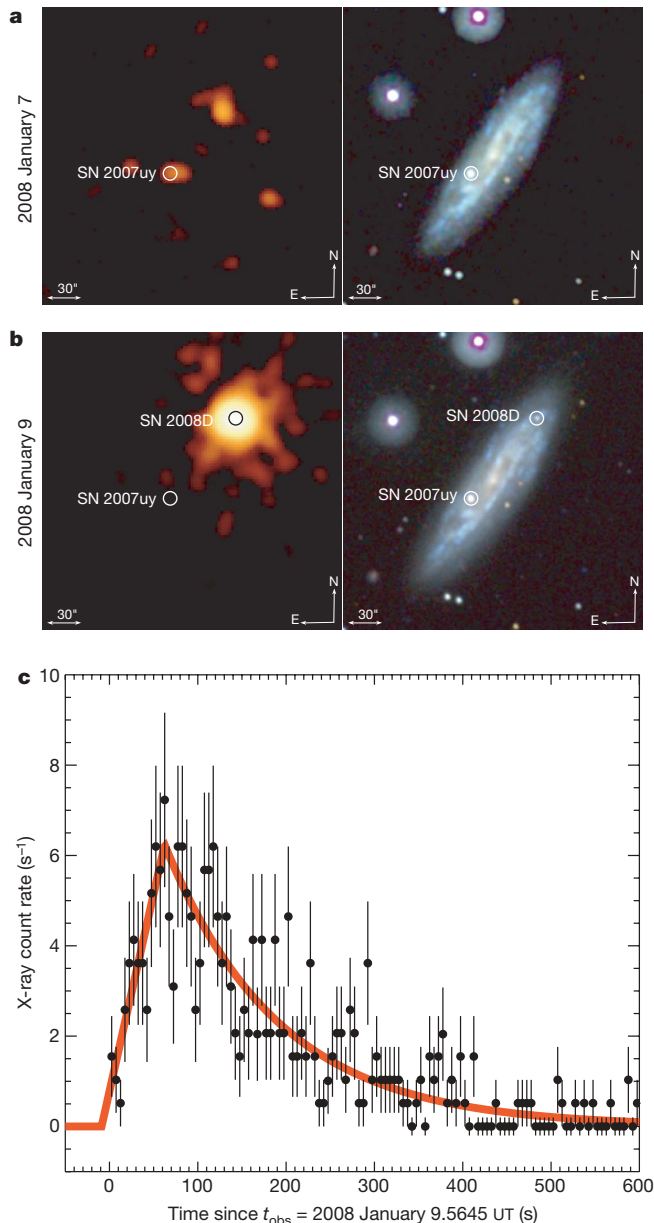


Figure 1 | Discovery image and X-ray light curve of XRO 080109/SN 2008D. **a**, X-ray (left) and ultraviolet (right) images of the field obtained on 2008 January 7 UT during Swift observations of the type Ibc supernova 2007uy. No source is detected at the position of SN 2008D to a limit of $\lesssim 10^{-3}$ counts s^{-1} in the X-ray band and $U \gtrsim 20.3$ mag. **b**, Repeated ultraviolet and X-ray observations of the field from January 9 UT during which we serendipitously discovered XRO 080109 and its ultraviolet counterpart. The position of XRO 080109 is right ascension $\alpha = 09$ h 09 min 30.70 s, declination $\delta = 33^{\circ} 08' 19.1''$ (J2000) ($\pm 3.5''$), about 9 kpc from the centre of NGC 2770. **c**, X-ray light curve of XRO 080109 in the 0.3–10 keV band. The data were accumulated in the photon counting mode and were processed using version 2.8 of the Swift software package, including the most recent calibration and exposure maps. The high count rate resulted in photon pile-up, which we correct for by fitting a King function profile to the point spread function (PSF) to determine the radial point at which the measured PSF deviates from the model. The counts were extracted using an annular aperture that excluded the affected 4 pixel core of the PSF, and the count rate was corrected according to the model. Error bars, $\pm 1\sigma$. Using a fast rise, exponential decay model (red curve), we determine the properties of the outburst, in particular its onset time, t_0 , which corresponds to the explosion time of SN 2008D. The best-fit parameters are a peak time of 63 ± 7 s after the beginning of the observation, an e-folding time of 129 ± 6 s, and peak count rate of 6.2 ± 0.4 counts s^{-1} (90% confidence level using Cash statistics). The best-fit value of t_0 is January 9 13:32:40 UT (that is, 9 s before the start of the observation) with a 90% uncertainty range of 13:32:20 to 13:32:48 UT.

Most importantly, the inferred rate of X-ray outbursts indicates that all core-collapse supernovae produce detectable shock break-out emission. Thus, we predict that future wide-field X-ray surveys will uncover hundreds of supernovae each year at the time of explosion, providing the long-awaited temporal and positional triggers for neutrino and gravitational wave searches.

Discovery of the X-ray outburst

On 2008 January 9 at 13:32:49 UT, we serendipitously discovered an extremely bright X-ray transient during a scheduled Swift X-ray Telescope (XRT) observation of the galaxy NGC 2770 (distance $d = 27$ Mpc). Previous XRT observations of the field just two days earlier revealed no pre-existing source at this location. The transient, hereafter designated as X-ray outburst (XRO) 080109, lasted about 400 s, and was coincident with one of the galaxy's spiral arms (Fig. 1). From observations described below, we determine that XRO 080109 is indeed located in NGC 2770, and we thus adopt this association from here on.

The temporal evolution is characterized by a fast rise and exponential decay, often observed for a variety of X-ray flare phenomena (Fig. 1). We determine the onset of the X-ray emission to be 9_{-8}^{+20} s before the beginning of the observation, implying an outburst start time (t_0) of January 9.5644 UT. The X-ray spectrum is best fitted by a power law ($N(E) \propto E^{-\Gamma}$, where N and E are the photon number and energy, respectively) with a photon index of $\Gamma = 2.3 \pm 0.3$, and a hydrogen column density of $N_H = 6.9_{-1.5}^{+1.8} \times 10^{21}$ cm^{-2} , in excess of the absorption within the Milky Way (see Supplementary Information). The inferred unabsorbed peak flux is $F_{X,p} \approx 6.9 \times 10^{-10}$ $\text{erg cm}^{-2} \text{s}^{-1}$ (0.3–10 keV). We also measure significant spectral softening during the outburst.

The XRO was in the field of view of the Swift Burst Alert Telescope (BAT; 15–150 keV) beginning 30 min before and continuing throughout the outburst, but no γ -ray counterpart was detected. Thus, the outburst was not a GRB (see also Supplementary Information). Integrating over the duration of the outburst, we place a limit on the γ -ray fluence of $f_\gamma \lesssim 8 \times 10^{-8}$ erg cm^{-2} (3σ), a factor of three times higher than an extrapolation of the X-ray spectrum to the BAT energy band.

The total energy of the outburst is thus $E_X \approx 2 \times 10^{46}$ erg, at least three orders of magnitude lower¹⁰ than GRBs. The peak luminosity is $L_{X,p} \approx 6.1 \times 10^{43}$ erg s^{-1} , several orders of magnitude larger than the Eddington luminosity (the maximum luminosity for a spherically accreting source) of a solar mass object, outbursts from ultra-luminous X-ray sources and type I X-ray bursts. In summary, the properties of XRO 080109 are distinct from those of all known X-ray transients.

The birth of a supernova

Simultaneous observations of the field with the co-aligned Ultraviolet/Optical Telescope (UVOT) on board Swift showed no evidence for a contemporaneous counterpart. However, UVOT observations just 1.4 h after the outburst revealed¹¹ a brightening ultraviolet/optical counterpart. Subsequent ground-based optical observations also uncovered^{11–13} a coincident source.

We promptly obtained optical spectroscopy of the counterpart with the Gemini North 8-m telescope beginning 1.74 d after the outburst (Fig. 2). The spectrum is characterized by a smooth continuum with narrow absorption lines of Na I (wavelengths 5,890 and 5,896 Å) at the redshift of NGC 2770. More importantly, we note broad absorption features near 5,200 and 5,700 Å and a drop-off beyond 7,000 Å, strongly suggestive of a young supernova. Subsequent observations confirmed these spectral characteristics^{11,14}, and the transient was classified^{11,15} as type Ibc SN 2008D based on the lack of hydrogen and weak silicon features.

Thanks to the prompt X-ray discovery, the temporal coverage of our optical spectra exceeds those of most supernovae, rivalling even the best-studied GRB-associated supernovae, and SN 1987A (Fig. 2). We see a clear evolution from a mostly featureless continuum to broad absorption lines, and finally to strong absorption features with moderate widths. Moreover, our spectra reveal the emergence of

strong He I features within a few days of the outburst (see also ref. 16). Thus, SN 2008D is a He-rich type Ibc supernova, unlike¹⁷ GRB-associated supernovae. Observations at high spectral resolution further reveal significant host galaxy extinction, with $A_V \approx 1.2$ – 2.5 mag (see Supplementary Information).

The well-sampled ultraviolet/optical light curves in ten broadband filters (2,000–10,000 Å) exhibit two distinct components (Fig. 3). First, an ultraviolet-dominated component that peaks about a day after the X-ray outburst, and which is similar to very early observations¹⁸ of the GRB-associated SN 2006aj. The second component is significantly redder and peaks on a timescale of about 20 d, consistent with observations of all type Ibc supernovae. Accounting for an extinction of $A_V = 1.9$ mag (Fig. 3), the absolute peak brightness of the second component is $M_V \approx -16.7$ mag, at the low end of the distribution¹⁹ for type Ibc supernovae and GRB-associated supernovae.

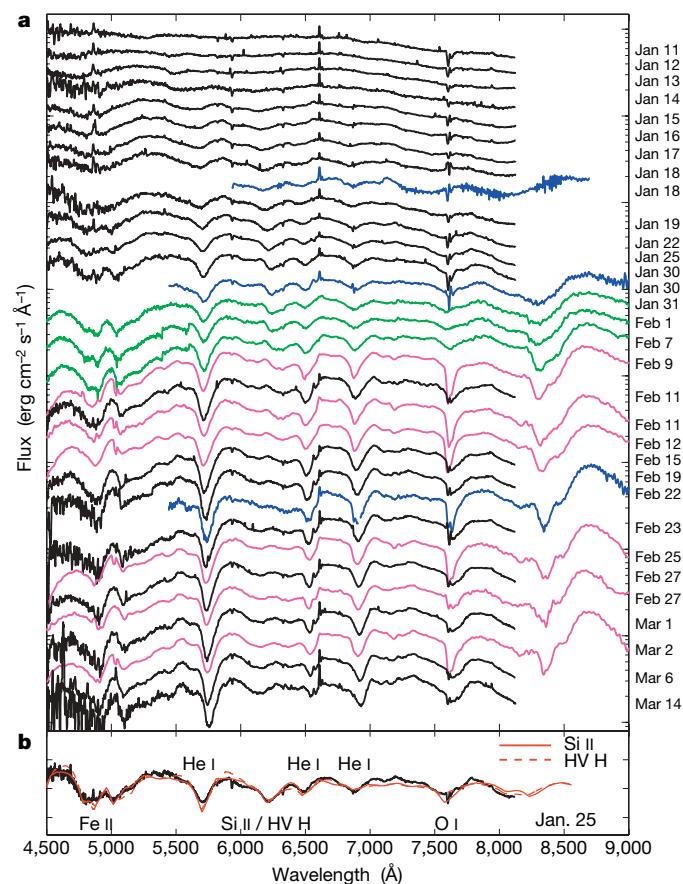


Figure 2 | Optical spectra of XRO 080109/SN 2008D, and model fit. a, The spectra are plotted logarithmically in flux units and shifted for clarity. **b**, A model fit to the January 25 UT spectrum using the spectral fitting code SYNOW. We identify several strong features attributed to He I, O I and Fe II, indicating a type Ibc classification. In addition, we find an absorption feature at 6,200 Å that can be identified as Si II or high velocity H I (HV H; see Supplementary Information for details). The observations were performed using the following facilities: The Gemini Multi-Object Spectrograph (GMOS) on the Gemini North 8-m telescope (black); the Dual Imaging Spectrograph (DIS) on the Apache Point 3.5-m telescope (blue); the Double Spectrograph (DBSP) on the Palomar Hale 200-inch telescope (green); and the Low Resolution Spectrograph (LRS) on the Hobby-Eberly 9.2-m telescope (magenta). The details of the observational set-up and the exposure times are provided in Supplementary Information. The data were reduced using the gemini package within the Image Reduction and Analysis Facility (IRAF) software for the GMOS data. All other observations were reduced using standard packages in IRAF. The supernova spectra were extracted from the two-dimensional data using a nearby background region to reduce the contamination from host galaxy emission. Absolute flux calibration was achieved using observations of the standard stars Feige 34 and G191B2B.

A shock break-out origin

As some type Ibc supernovae harbour GRBs, we investigate the possibility that the XRO is produced by a relativistic outflow. In this scenario, the X-ray flux and simultaneous upper limits in the ultraviolet/optical require the outflow to be ultra-relativistic with a bulk Lorentz factor $\gamma \approx 90$, but its radius to be only $R \approx 10^{10}$ cm; here $\gamma \equiv (1 - \beta^2)^{-1/2}$ and $\beta \equiv v/c$, where v is the outflow velocity and c is the speed of light. However, given the observed duration of the outburst, we expect²⁰ $R \approx 4\gamma^2 ct \approx 10^{17}$ cm, indicating that the relativistic outflow scenario is not self-consistent (see Supplementary Information for details).

We are left with a trans- or non-relativistic origin for the outburst, and we consider supernova shock break-out as a natural scenario. The break-out is defined by the transition from a radiation-mediated to a collisional (or collisionless²¹) shock as the optical depth of the outflow decreases to unity. Such a transition has long been predicted^{4,5} to produce strong, thermal ultraviolet/X-ray emission at

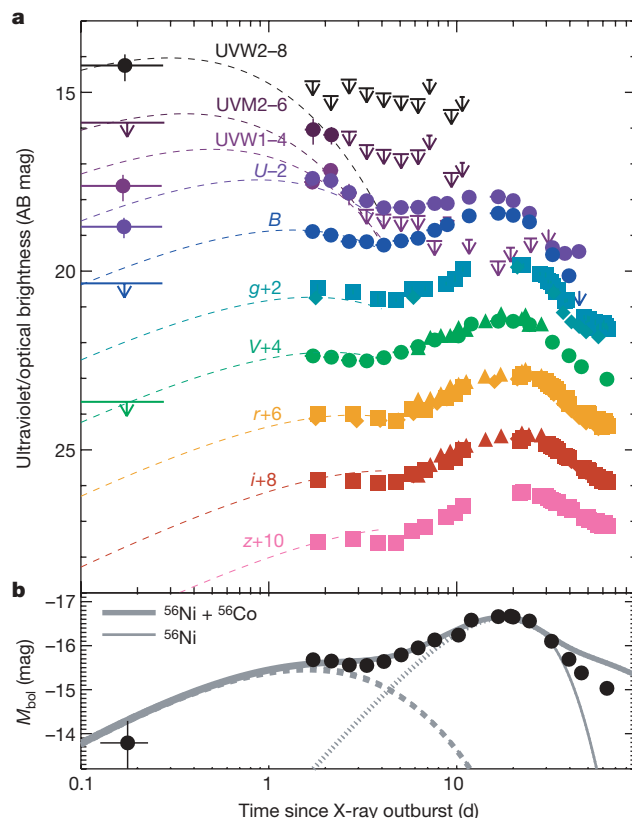


Figure 3 | Optical and ultraviolet light curves of XRO 080109/SN 2008D, and model fit. a, Optical and ultraviolet light curves. Data are from Swift UVOT (circles), Palomar 60-inch telescope (squares), Gemini/GMOS (diamonds), and the SLOTTIS telescope (triangles). Tables summarizing the observations and data analysis are available in Supplementary Information. The data have not been corrected for host galaxy extinction and have been offset (as labelled) for clarity. We fit the data before 3 d with a cooling envelope blackbody emission model⁶ (dashed lines) that accounts for host extinction (A_V). We find a reasonable fit to the data with $R_* \approx 10^{11}$ cm, $E_K \approx 2 \times 10^{51}$ erg, $M_{ej} \approx 5 M_\odot$ and $A_V \approx 1.9$ mag, consistent with the constraints from the high-resolution optical spectrum. The radius and temperature of the photosphere at 1 d are $R_{ph} \approx 3 \times 10^{14}$ cm and $T_{ph} \approx 10^4$ K, respectively. Error bars are 1σ ; down-pointing arrows are upper limits (3σ). **b**, The absolute bolometric magnitude light curve (corrected for host extinction). The dashed lines are the same cooling envelope model described above, while the short-dashed lines are models of supernova emission powered by radioactive decay. The solid lines are combined models taking into account the decay of ^{56}Ni (thin line) and $^{56}\text{Ni} + ^{56}\text{Co}$ (thick line). The supernova models provide an independent measure of E_K and M_{ej} , as well as M_{Ni} (see Supplementary Information for a detailed discussion of the models). We find values that are consistent to within 30% with those inferred from the cooling envelope model.

the time of explosion. A non-thermal component at higher energies may be produced²² by multiple scatterings of the photons between the ejecta and a dense circumstellar medium (bulk comptonization).

We attribute the observed non-thermal outburst to comptonized emission from shock break-out, indicating that the associated thermal component must lie below the XRT low energy cut-off, ~ 0.1 keV. With the reasonable assumption that the energy in the thermal (E_{th}) and comptonized components is comparable, we constrain⁶ the radius at which shock break-out occurs to $R_{\text{sbo}} \gtrsim 7 \times 10^{11} (T)^{-4/7} (E_X)^{3/7}$ cm (here T is in units of 0.1 keV, and E_X in units of 2×10^{46} erg). This is consistent with a simple estimate derived from the rise time of the outburst, $R_{\text{sbo}} = c\delta t \approx 10^{12}$ cm, and larger than the typical radii of Wolf-Rayet stars²³, $\sim 10^{11}$ cm. We therefore attribute the delayed shock break-out to the presence of a dense stellar wind, similar^{6,18} to the case of the GRB-associated supernova SN 2006aj.

The shock velocity at break-out is⁶ $(\gamma\beta) \lesssim 1.1$ and the outflow is thus trans-relativistic, as expected²⁴ for a compact progenitor. Using these constraints, the inferred optical depth of the ejecta to thermal X-rays is $\tau_{\text{ej}} \approx 1.5 (E_X) (R_{\text{sbo}})^{-2} (\gamma - 1)^{-1} \approx 3$ (here E_X is normalized as above, and R_{sbo} is in units of 7×10^{11} cm), and comptonization is thus efficient, confirming our model. Equally important, as the ejecta expand outward the optical depth of the stellar wind decreases and the spectrum of the comptonized emission is expected²² to soften, in agreement with the observed trend.

The shock break-out emission traces the wind mass-loss rate of the progenitor, \dot{M} , in the final hours leading up to the explosion. The inferred density indicates $\dot{M} \approx 4\pi v_w R_{\text{sbo}} / \kappa \approx 10^{-5} M_{\odot} \text{ yr}^{-1}$; here $\kappa \approx 0.4 \text{ cm}^2 \text{ g}^{-1}$ is the Thomson opacity for an ionized hydrogen wind and $v_w \approx 10^3 \text{ cm s}^{-1}$ is the typical⁷ wind velocity for Wolf-Rayet stars. The mass-loss rate is consistent⁷ with the average values inferred for Galactic Wolf-Rayet stars, and, along with the inferred compact stellar radius and the lack of hydrogen features, leads us to conclude that the progenitor was a Wolf-Rayet star.

Two ultraviolet/optical emission components

The early ultraviolet/optical emission ($t \lesssim 3$ d, where t is time since t_0) appears to be a distinct component, based on its different temporal behaviour and bluer colours (Fig. 3). We attribute this early emission to cooling of the outer stellar envelope following the passage of the shock through the star and its subsequent break-out (marked by the X-ray outburst). The expected blackbody radiation is characterized⁶ by the photospheric radius and temperature, which evolve with t respectively as $R_{\text{ph}} \propto t^{0.8}$ and $T_{\text{ph}} \propto t^{-0.5}$, and depend on the total ejecta kinetic energy (E_K) and mass (M_{ej}), and on the stellar radius before the explosion (R_*).

The model light curves provide a good fit to the early ultraviolet/optical data (Fig. 3). The implied stellar radius is $R_* \approx 7 \times 10^{10}$ cm, consistent with that expected²³ for a Wolf-Rayet progenitor. Moreover, this value is smaller than the shock break-out radius, confirming our earlier inference that the break-out occurs in the extended stellar wind.

The ratio of E_K and M_{ej} also determines the shape of the main supernova light curve (see, for example, ref. 25), and the mass of ^{56}Ni synthesized in the explosion (M_{Ni}) determines²⁶ its peak optical luminosity. To break the degeneracy between E_K and M_{ej} , we measure the photospheric velocity from the optical spectra at maximum light, $v_{\text{ph}} = 0.3 (E_K/M_{\text{ej}})^{1/2} \approx 11,500 \text{ km s}^{-1}$; this is comparable to that of ordinary type Ibc supernovae, but somewhat slower¹⁷ than GRB-associated supernovae (Fig. 2 and Supplementary Information). We find that both light curve components are self-consistently fitted with $E_K \approx (2-4) \times 10^{51} \text{ erg}$, $M_{\text{ej}} \approx 3-5 M_{\odot}$, and $M_{\text{Ni}} \approx 0.05-0.1 M_{\odot}$ (Fig. 3).

Long-lived X-ray and radio emission

Whereas ultraviolet/optical observations probe the bulk material, radio and X-ray emission trace fast ejecta. Our Swift follow-up observations of the XRO revealed fainter X-ray emission several hours after

the explosion, with $L_X \approx 2 \times 10^{40} \text{ erg s}^{-1}$ ($t \approx 0.2$ d). This emission exceeds the extrapolation of the outburst by many orders of magnitude, indicating that it is powered by a different mechanism. Using a high-angular-resolution observation from the Chandra X-ray Observatory on January 19.86 UT, we detect the supernova with a luminosity $L_X = (1.0 \pm 0.3) \times 10^{39} \text{ erg s}^{-1}$ (0.3–10 keV), and further resolve three nearby sources contained within the 18-arcsec resolution element of XRT. Correcting all XRT observations for these sources, we find that the long-lived X-ray emission decays steadily as $F_X \propto t^{-0.7}$ (Supplementary Information).

Using the Very Large Array (VLA) on January 12.54 UT, we further discovered a new radio source at the position of the supernova that was not present on January 7 UT. Follow-up observations were obtained at multiple frequencies between 1.4 and 95 GHz using the VLA, the Combined Array for Research in Millimeter-wave Astronomy (CARMA) and the Very Long Baseline Array (VLBA).

The broadband radio emission on January 14 UT reveals a spectral peak, $\nu_p \approx 43$ GHz, with a flux density, $F_{\nu,p} \approx 4 \text{ mJy}$, and a low frequency spectrum, $F_{\nu} \propto \nu^{-2.5}$. Subsequent observations show that ν_p cascades to lower frequencies, similar to the evolution observed in other type Ibc supernovae (see, for example, ref. 27). The passage of ν_p through each frequency produces a light curve peak. We measure $F_{\nu} \propto t^{1.4}$ and $F_{\nu} \propto t^{-1.2}$ for the light curve rise and decline, respectively (Fig. 4).

We note that our X-ray and radio observations of SN 2008D are the earliest ever obtained for a normal type Ibc supernova. At $t \approx 10$ d, the X-ray and peak radio luminosities are several orders of magnitude lower^{28,29} than those of GRB afterglows but comparable^{30,31} to those of normal type Ibc supernovae.

The properties of the fast ejecta

Radio synchrotron emission is produced³² by relativistic electrons accelerated in the supernova shock as they gyrate in the amplified magnetic field. Self-absorption suppresses the spectrum below the peak to $F_{\nu} \propto \nu^{2.5}$, in excellent agreement with our observations. In this context, we infer^{33,34} the radius of the fast ejecta, using the measured ν_p and $L_{\nu,p}$, to be $R \approx 3 \times 10^{15}$ cm at $t \approx 5$ d. The implied mean velocity is $\beta \approx 0.25$, clearly ruling out relativistic ejecta.

With this conclusion there are two possibilities for the ejecta dynamics. First, the supernova may be in free expansion, $R \propto t$, consistent with observations of type Ibc supernovae (see, for example, ref. 27). Alternatively, the ejecta may have been relativistic at early time and then rapidly decelerated, leading to $R \propto t^{2/3}$. In the latter scenario, the dynamics are governed³⁵ by the Sedov-Taylor solution. As discussed in Supplementary Information, the temporal evolution of the radio light curves is clearly inconsistent with the Sedov-Taylor model, ruling out even early relativistic expansion.

Thus, the radio emission is produced by freely expanding ejecta, indicative of the broad velocity structure expected²⁴ for ordinary core-collapse supernovae. The standard formulation²⁷ provides an excellent fit to the data (Fig. 4) and indicates that the energy coupled to fast material is $E_{\text{K,R}} \approx 10^{48}$ erg (here subscript K,R indicates kinetic energy probed by radio observations), just 0.1% of the total kinetic energy. Moreover, the inferred density profile is $\rho(r) \propto r^{-2}$ (where r is the radius from the explosion site), as expected for a steady stellar wind. The inferred mass-loss rate, $\dot{M} \approx 7 \times 10^{-6} M_{\odot} \text{ yr}^{-1}$, is in agreement with our shock break-out value, indicating a stable mass loss rate in the final ~ 3 yr to ~ 3 h of the progenitor's life.

The radio-emitting electrons also account for the late X-ray emission through their inverse Compton (IC) upscattering of the supernova optical photons (with a luminosity L_{opt}). The expected⁶ X-ray luminosity is $L_{\text{IC}} \approx 3 \times 10^{39} (E_{\text{K,R}}/L_{\text{opt}})(t)^{-2/3} \text{ erg s}^{-1}$ (where $E_{\text{K,R}}$ is units of 10^{48} erg, L_{opt} in $10^{42} \text{ erg s}^{-1}$, and t in days), in excellent agreement with the observations by XRT and the Chandra X-ray Observatory. We note that the synchrotron contribution in the X-ray band is lower by at least two orders of magnitude.

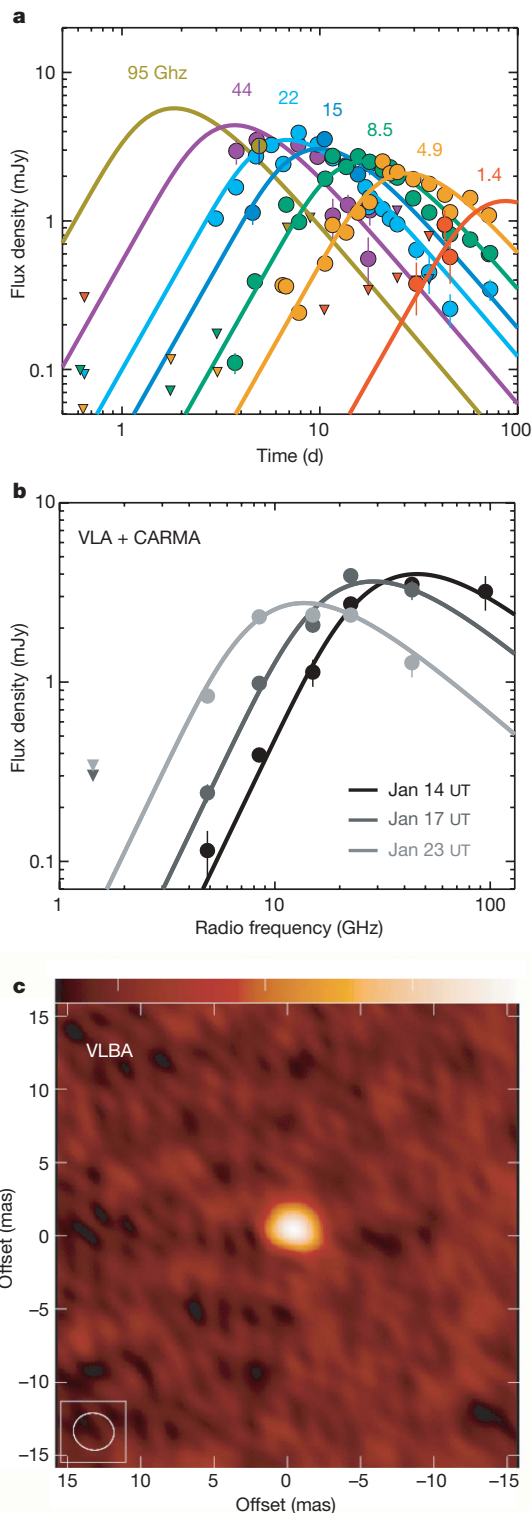


Figure 4 | Radio light curves, spectra and image of XRO 080109/SN 2008D. Radio data from 1.4 to 95 GHz were obtained with the VLA, CARMA and the VLBA (circles are detections and inverted triangles represent 3σ upper limits). Error bars are 1σ. The flux measurements and a description of the data analysis are provided in Supplementary Information. **a**, Radio light curves with a model of synchrotron self-absorbed emission arising²⁷ from shocked material surrounding the freely expanding supernova. We adopt a shock compression factor of η = 4 for the post-shock material and assume that the electrons and magnetic fields each contribute 10% to the total post-shock energy density. The best-fit model (solid lines) implies the following physical parameters and temporal evolution: $R \approx 3 \times 10^{15}(t)^{0.9}$ cm, $E_{K,R} \approx 10^{48}(t)^{0.8}$ erg and $B \approx 2.4(t)^{-1}$ G, where B is the magnetic field strength (here t is in units of 5 d). The implied density profile is $\rho(r) \propto r^{-2}$, as expected for the wind from a massive star. **b**, Broadband radio spectra. The spectral peak of the radio synchrotron emission cascades to lower frequencies over the course of our follow-up observations with $\nu_p \propto t^{-1}$. The low frequency turn-over is consistent with expectations for synchrotron self-absorption (grey lines). **c**, Radio image from a VLBA observation on February 8 UT. The colour scale goes from -0.2 mJy per beam (black) to 1.4 mJy per beam (white). We place an upper limit on the angular size of the ejecta of 1.2 mas (3σ), corresponding to a physical radius of $\lesssim 2.4 \times 10^{17}$ cm. This limit is a factor of 16 times larger than, and therefore consistent with, the radius derived from the radio supernova model. However, it places a limit of $(\gamma\beta) \lesssim 3$ on the expansion velocity.

about two years. Along with the XRT field of view (24 arcmin on a side), the number density of L_* galaxies ($\phi \approx 0.05 L_* \text{ Mpc}^{-3}$), and the detectability limit of XRT for events like XRO 080109 ($d \lesssim 200$ Mpc), we infer an XRO rate of $\gtrsim 10^{-3} L_*^{-1} \text{ yr}^{-1}$ (95% confidence level, Fig. 5); here L_* is the characteristic luminosity of galaxies³⁷. This rate is at least an order of magnitude larger than for GRBs^{38,39}. On the other hand, with a core-collapse supernova rate⁴⁰ of $10^{-2} L_* \text{ yr}^{-1}$, the probability of detecting at least one XRO if all such supernovae produce an outburst is about 50%.

We find a similar agreement with the supernova rate using the sensitivity of the BAT. The estimated³⁹ peak photon flux of the outburst is $0.03 \text{ cm}^{-2} \text{ s}^{-1}$ (1–1,000 keV), which for a 10^2 s image trigger⁴¹ is detectable to about 20 Mpc. The BAT on-sky monitoring time of 3 yr and the 2 sr field of view thus yield an upper limit on the XRO rate of $\lesssim 10^5 \text{ Gpc}^{-3} \text{ yr}^{-1}$, consistent with the core-collapse supernova rate⁴² of $6 \times 10^4 \text{ Gpc}^{-3} \text{ yr}^{-1}$.

Finally, we note that neither the late X-ray emission nor the radio emission show evidence for a rising component that could be attributed³⁶ to an off-axis GRB jet spreading into our line of sight. This conclusion is also supported by the unresolved size of the radio supernova from VLBA observations at $t \approx 1$ month, $R \lesssim 2.4 \times 10^{17}$ cm (3σ), which constrains the outflow velocity to be $\gamma\beta \lesssim 3$.

The rate of XROs

To estimate the rate of XROs, we find that the on-sky effective monitoring time of the XRT from the launch of Swift through to the end of January 2008, including only those exposures longer than 300 s, is

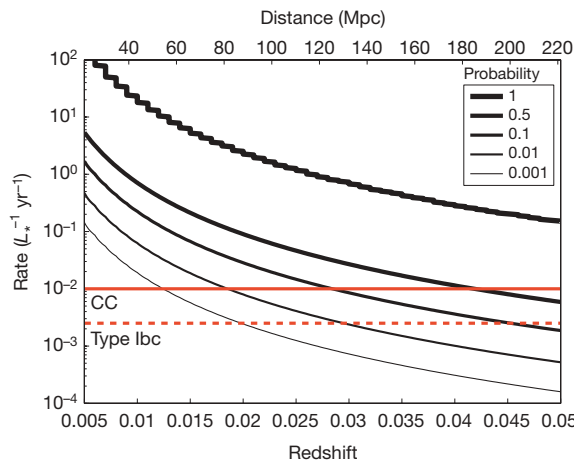


Figure 5 | Volumetric rate of X-ray outbursts similar to XRO 080109. We use all XRT observations longer than 300 s along with the field of view (24 arcmin on a side), the number density of L_* galaxies ($\phi \approx 0.05 L_* \text{ Mpc}^{-3}$), and the detectability limit of XRT for events like XRO 080109 ($d \lesssim 200$ Mpc). The curves indicate the rate ($L_*^{-1} \text{ Mpc}^{-3} \text{ yr}^{-1}$) inferred from one detection in a total of about 2 yr of effective on-sky XRT observations as a function of the distance to which XROs can be detected. Also shown are the rates⁴⁰ of core-collapse supernovae (CC; solid horizontal line) and type Ibc supernovae (dashed horizontal line) as determined from optical supernova searches. The rate of events like XRO 080109 is consistent with the core-collapse rate at the 50% probability level.

Finally, we note that NGC 2770 hosted an unusually high rate of three type Ibc supernovae in the past 10 yr. However, the galaxy has a typical luminosity ($0.3 L_*$) and a total star formation rate of only $0.5\text{--}1 M_\odot \text{ yr}^{-1}$ (see Supplementary Information), two orders of magnitude lower than the extreme starburst galaxy Arp 220, which has⁴³ a supernova rate of $4 \pm 2 \text{ yr}^{-1}$. The elevated supernova rate in NGC 2770, with a chance probability of $\sim 10^{-4}$, may simply be a statistical fluctuation, given the sample of $\sim 4 \times 10^3$ known supernova host galaxies. Alternatively, it may point to a recent episode of increased star formation activity, perhaps triggered by interaction with the companion galaxy NGC 2770B at a separation⁴⁴ of only 22 kpc.

Implications for supernova progenitors

Our observations probe the explosion ejecta over a wide range in velocity, $\sim 10,000\text{--}210,000 \text{ km s}^{-1}$. Taken together, the material giving rise to the X-ray outburst, the radio emission, and the optical light traces an ejecta profile of $E_K \propto (\gamma\beta)^{-4}$ up to trans-relativistic velocities. This profile is in good agreement with theoretical expectations²⁴ for a standard hydrodynamic spherical explosion of a compact star, but much steeper³⁹ than for relativistic GRB-associated supernovae.

On the other hand, we note the similarity between the shock break-out properties of the He-rich SN 2008D and the He-poor GRB-associated SN 2006aj, both suggestive of a dense stellar wind around a compact Wolf-Rayet progenitor. In the context of type Ibc supernovae and GRB progenitors, this provides evidence for continuity (and probably a single progenitor system) between He-rich and He-poor explosions, perhaps including GRBs.

Looking forward, our inference that every core-collapse supernova is marked by an XRO places the discovery and study of supernovae on the threshold of a major change. An all-sky X-ray satellite with a sensitivity similar to that of the Swift/XRT would detect and localize several hundred core-collapse supernovae per year, even if they are obscured by dust, at the time of explosion. As we have shown here, this would enable a clear mapping between the properties of the progenitors and those of the supernovae. Most important, however, X-ray outbursts will provide an unprecedented positional and temporal trigger for neutrino and gravitational wave detectors (such as IceCube and Advanced LIGO), which may ultimately hold the key to unlocking the mystery of the supernova explosion mechanism, and perhaps the identity of the compact remnants.

Received 11 February; accepted 4 April 2008.

1. Woosley, S. E. & Weaver, T. A. The physics of supernova explosions. *Annu. Rev. Astron. Astrophys.* **24**, 205–253 (1986).
2. Filippenko, A. V. Optical spectra of supernovae. *Annu. Rev. Astron. Astrophys.* **35**, 309–355 (1997).
3. Arnett, W. D., Bahcall, J. N., Kirshner, R. P. & Woosley, S. E. Supernova 1987A. *Annu. Rev. Astron. Astrophys.* **27**, 629–700 (1989).
4. Colgate, S. A. Early gamma rays from supernovae. *Astrophys. J.* **187**, 333–336 (1974).
5. Klein, R. I. & Chevalier, R. A. X-ray bursts from Type II supernovae. *Astrophys. J.* **223**, L109–L112 (1978).
6. Waxman, E., Mészáros, P. & Campana, S. GRB 060218: A relativistic supernova shock breakout. *Astrophys. J.* **667**, 351–357 (2007).
7. Cappa, C., Goss, W. M. & van der Hucht, K. A. A Very Large Array 3.6 centimeter continuum survey of galactic Wolf-Rayet stars. *Astrophys. J.* **127**, 2885–2897 (2004).
8. Woosley, S. E., Hegar, A. & Weaver, T. A. The evolution and explosion of massive stars. *Astrophys. J.* **74**, 1015–1071 (2002).
9. MacFadyen, A. I., Woosley, S. E. & Hegar, A. Supernovae, jets, and collapsars. *Astrophys. J.* **550**, 410–425 (2001).
10. Soderberg, A. M. et al. The sub-energetic γ -ray burst GRB 031203 as a cosmic analogue to the nearby GRB 980425. *Nature* **430**, 648–650 (2004).
11. Page, K. L. et al. Observations of an X-ray transient in NGC 2770. *GCN Rep.* **110** (2008).
12. Deng, J. & Zhu, Y. Bright X-ray transient (a XRF?) in NGC 2770 – a SN optical counterpart? *GCN Circ.* 7160 (2008).
13. Valenti, S., Turatto, M., Navasardyan, H., Benetti, S. & Cappellaro, E. Early OT detection of XRF in NGC 2770 in asiago frames. *GCN Circ.* 7163 (2008).
14. Malesani, D. et al. Transient in NGC 2770: Spectroscopic evidence for a SN. *GCN Circ.* 7169 (2008).
15. Li, W. & Filippenko, A. V. Supernova 2008D in NGC 2770. *Cent. Bur. Electron. Teleg.* 1202 (2008).

16. Modjaz, M. et al. Supernova 2008D in NGC 2770. *Cent. Bur. Electron. Teleg.* 1222 (2008).
17. Pian, E. et al. An optical supernova associated with the X-ray flash XRF 060218. *Nature* **442**, 1011–1013 (2006).
18. Campana, S. et al. The association of GRB 060218 with a supernova and the evolution of the shock wave. *Nature* **442**, 1008–1010 (2006).
19. Soderberg, A. M. et al. An HST study of the supernovae accompanying GRB 040924 and GRB 041006. *Astrophys. J.* **636**, 391–399 (2006).
20. Sari, R., Piran, T. & Narayan, R. Spectra and light curves of gamma-ray burst afterglows. *Astrophys. J.* **497**, 17–20 (1998).
21. Waxman, E. & Loeb, A. TeV neutrinos and GeV photons from shock breakout in supernovae. *Phys. Rev. Lett.* **87**, 071101 (2001).
22. Wang, X.-Y., Li, Z., Waxman, E. & Mészáros, P. Nonthermal gamma-ray/X-ray flashes from shock breakout in gamma-ray burst-associated supernovae. *Astrophys. J.* **664**, 1026–1032 (2007).
23. Moffat, A. F. J., Drissen, L. & Robert, C. in *Physics of Luminous Blue Variables* (eds Davidson, K., Moffat, A. F. J. & Lamers, H. J. G. L. M.) 229–237 (IAU Colloq. 113, Kluwer Academic, Dordrecht, 1989).
24. Matzner, C. D. & McKee, C. F. The expulsion of stellar envelopes in core-collapse supernovae. *Astrophys. J.* **510**, 379–403 (1999).
25. Valenti, S. et al. The broad-lined Type Ic supernova 2003jd. *Mon. Not. R. Astron. Soc.* **383**, 1485–1500 (2008).
26. Arnett, W. D. Type I supernovae. I – Analytic solutions for the early part of the light curve. *Astrophys. J.* **253**, 785–797 (1982).
27. Soderberg, A. M. et al. The radio and X-ray-luminous Type Ibc supernova 2003L. *Astrophys. J.* **621**, 908–920 (2005).
28. Berger, E., Kulkarni, S. R. & Frail, D. A. A standard kinetic energy reservoir in gamma-ray burst afterglows. *Astrophys. J.* **590**, 379–385 (2003).
29. Frail, D. A., Kulkarni, S. R., Berger, E. & Wieringa, M. H. A complete catalog of radio afterglows: The first five years. *Astron. J.* **125**, 2299–2306 (2003).
30. Berger, E., Kulkarni, S. R., Frail, D. A. & Soderberg, A. M. A radio survey of Type Ib and Ic supernovae: Searching for engine-driven supernovae. *Astrophys. J.* **599**, 408–418 (2003).
31. Kouveliotou, C. et al. Chandra observations of the X-ray environs of SN 1998bw/GRB 980425. *Astrophys. J.* **608**, 872–882 (2004).
32. Chevalier, R. A. Self-similar solutions for the interaction of stellar ejecta with an external medium. *Astrophys. J.* **258**, 790–797 (1982).
33. Readhead, A. C. S. Equipartition brightness temperature and the inverse Compton catastrophe. *Astrophys. J.* **426**, 51–59 (1994).
34. Kulkarni, S. R. et al. Radio emission from the unusual supernova 1998bw and its association with the γ -ray burst of 25 April 1998. *Nature* **395**, 663–669 (1998).
35. Waxman, E. The nature of GRB 980425 and the search for off-axis gamma-ray burst signatures in nearby Type Ib/c supernova emission. *Astrophys. J.* **602**, 886–891 (2004).
36. Soderberg, A. M., Nakar, E., Berger, E. & Kulkarni, S. R. Late-time radio observations of 68 Type Ibc supernovae: Strong constraints on off-axis gamma-ray bursts. *Astrophys. J.* **638**, 930–937 (2006).
37. Blanton, M. R. et al. The galaxy luminosity function and luminosity density at redshift $z = 0.1$. *Astrophys. J.* **592**, 819–838 (2003).
38. Schmidt, M. Luminosity function of gamma-ray bursts derived without benefit of redshifts. *Astrophys. J.* **552**, 36–41 (2001).
39. Soderberg, A. M. et al. Relativistic ejecta from X-ray flash XRF 060218 and the rate of cosmic explosions. *Nature* **442**, 1014–1017 (2006).
40. Cappellaro, E., Evans, R. & Turatto, M. A new determination of supernova rates and a comparison with indicators for galactic star formation. **351**, 459–466 (1999).
41. Band, D. L. Postlaunch analysis of Swift's gamma-ray burst detection sensitivity. *Astrophys. J.* **644**, 378–384 (2006).
42. Dahlen, T. et al. High-redshift supernova rates. *Astrophys. J.* **613**, 189–199 (2004).
43. Lonsdale, C. J., Diamond, P. J., Thrall, H., Smith, H. E. & Lonsdale, C. J. VLBI images of 49 radio supernovae in Arp 220. *Astrophys. J.* **647**, 185–193 (2006).
44. Fynbo, J. P. U., Malesani, D., Augusteijn, T. & Niemi, S.-M. NGC 2770B has the same redshift as NGC 2770. *GCN Circ.* 7186 (2008).

Supplementary Information is linked to the online version of the paper at www.nature.com/nature.

Acknowledgements This Article is based in part on observations obtained at the Gemini Observatory through the Director's Discretionary Time. Gemini is operated by the Association of Universities for Research in Astronomy, Inc., under a cooperative agreement with the NSF on behalf of the Gemini partnership: the NSF (US), the STFC (UK), the NRC (Canada), CONICYT (Chile), the ARC (Australia), CNPq (Brazil) and SECYT (Argentina). The VLA is operated by NRAO, a facility of the NSF operated under cooperative agreement by Associated Universities, Inc. Some of the data presented herein were obtained at the W. M. Keck Observatory, which is operated as a scientific partnership among the California Institute of Technology, the University of California and NASA. The Observatory was made possible by the financial support of the W. M. Keck Foundation. A.M.S. acknowledges support by NASA through a Hubble Fellowship.

Author Information Reprints and permissions information is available at www.nature.com/reprints. Correspondence and requests for materials should be addressed to A.M.S. (alicia@astro.princeton.edu).